Journal Name

ARTICLE TYPE

Cite this: DOI: 10.1039/xxxxxxxxxx

Insights into the Structural Dynamics of Poly Lactic-co-glycolic Acid at Terahertz Frequencies

Talia A. Shmool,[a] J. Axel Zeitler,[a*]

Received Date
Accepted Date

DOI: 10.1039/xxxxxxxxxx

www.rsc.org/journalname

The mechanical properties of an amorphous copolymer are directly related to the dynamic processes occurring at the molecular level. Poly lactic-co-glycolic acid (PLGA) is a biodegradable copolymer, and in this work we investigate the dynamics of PLGA and its glass transition behaviour by performing variable temperature terahertz time-domain spectroscopy (THz-TDS) experiments. We correlate PLGA dynamics, as measured at terahertz frequencies, their temperature dependence, molecular weight (MW), lactide to glycolide ratio, and free volume. The THz-TDS data can be used to detect two distinct transition processes, T_β and $T_{g,\alpha}$. To complement our analysis, we use dynamic mechanical analysis (DMA) to probe the β- and α-relaxation processes in PLGA, and compare the results obtained from the DMA experiments with those obtained using THz-TDS. The values of $T_{g,\alpha}$, as determined from the THz-TDS experiments, are in good agreement with $T_{g,\mathrm{DSC}}$, determined by calorimetric measurements, and with $T_{g,\mathrm{DMA}}$, determined by the DMA measurements. We attribute T_β to the change in dipole moments associated with the β-relaxation process, originating from the local rotation of C-O macromolecular chain segments, and $T_{g,\alpha}$ to the change in dipole moments due to large segmental motion of the copolymer backbone associated with the α-relaxation process. By showing experimental temperature-dependent results from THz-TDS and DMA for PLGA, we demonstrate that the behaviour of PLGA is in line with the potential energy surface interpretation by Goldstein as well as the free volume theory of Fox and Flory, and that both concepts together can be used to understand amorphous polymers.

For a given amorphous polymer the glass transition process, and the molecular dynamics leading up to this event, play a key role for its chemical stability as well as its physical and mechanical properties[1–3]. It has been widely reported that many amorphous polymers exhibit at least two dielectric relaxation processes: the primary, or α-relaxation process, that can be observed at temperatures above the glass transition temperature, T_g or $T_{g,\alpha}$, and the secondary, or β-relaxation process, which occurs at temperatures below T_g and is associated with a secondary process at T_β[4–8]. The α-relaxation process is the central structural relaxation in polymers and is associated with segmental relaxation motions of a polymer molecule[5,9]. However, to date, the origin and molecular mechanisms associated with the α- and β-relaxation processes in amorphous polymers remain relatively poorly understood.

A number of experimental studies have demonstrated that the dielectric loss peak that is characteristic of the β-relaxation process spans a wide range of frequencies. It has been suggested that, depending on the polymer, the β-relaxation process can be attributed to the re-orientational motions of a side group or the local motions of the polymer chain backbone, which is independent of the cooperative motion of surrounding chains[10,11]. In polymer systems, more than one secondary relaxation can exist. It is worth highlighting the Johari-Goldstein (JG) β-relaxation, sometimes also referred to in the literature as the slow β-relaxation[12,13]. The JG β-relaxation is considered a universal feature of all disordered materials, and, like all higher order relaxation processes, is observed at higher frequencies than the α-relaxation. For a long time there has been a lively discussion regarding the exact physical nature of the higher order relaxation processes and whether such processes are indeed distinctly different from one another. Given this situation, it is not surprising that the terminology of the secondary relaxation processes mostly depends on the traditions developed by each respective community. It is sometimes suggested that the JG β-relaxation process relates to intermolecular degrees of freedom, in contrast to the general β-relaxation process which is intramolecular in nature[1,4,12]. Such a view is in direct contrast to the more nuanced potential energy surface (PES) model proposed by Goldstein almost half a century ago[14]. Recent experimental and theoretical work clearly highlights that

[a] *Department of Chemical Engineering and Biotechnology, University of Cambridge, Philippa Fawcett Drive, Cambridge CB3 0AS, United Kingdom; E-mail:jaz22@cam.ac.uk*

† Electronic Supplementary Information (ESI) available: [details of any supplementary information available should be included here]. See DOI: 10.1039/b000000x/

the PES approach is the most intuitive and comprehensive model to understand the molecular dynamics in disordered systems and that intra- and intermolecular processes are always fundamentally coupled by means of the PES.[15]

The vibrational modes of polylactic acid (PLA) and polyglycolic acid (PGA) have been investigated in the literature using a wide range of techniques, including terahertz spectroscopy, Raman and far-infrared (FIR) spectroscopy, and quantum mechanical calculations[16–18]. For example, it has been shown that with increasing temperature the intermolecular interactions of PGA can change, as the C=O group of PGA shifts from 2.1 THz to a lower frequency[18]. Furthermore, the role of steric effects, specifically between a carbonyl oxygen atom and a H-C bond has been investigated for PGA[18]. Poly lactic-co-glycolic acid (PLGA) is a copolymer of PLA and PGA[19]. PLGA is a biodegradable and biocompatible copolymer with widespread biomedical applications. It is soluble in a wide range of solvents and is thermally stable, with no appreciable weight loss observed at temperatures below $473-523\,\mathrm{K}$. While the overall mechanical properties of PLGA have been investigated in detail[20] the relaxation properties of the material are less well understood, and there is a gap in the existing literature, since PLGA has yet to be investigated at terahertz frequencies.

Detecting the α- and β-relaxation processes can be achieved using various techniques, such as Brillouin light scattering, neutron scattering, dynamic mechanical analysis (DMA), Raman spectroscopy, dielectric spectroscopy, and THz-TDS[21–25]. Terahertz time-domain spectroscopy (THz-TDS) is a relatively recent technique that can be used to investigate the molecular dynamics of relaxation processes at high frequencies[26]. It is a non-contact technique which can be used to measure polymer mobility over a broad temperature range at frequencies of $0.1-3\,\mathrm{THz}$ and can be applied to investigate the microscopic mechanisms of amorphous polymer dynamics[27]. Using THz-TDS we previously showed that a sub-T_g transition can be found in organic molecular glasses[24]. The behaviour of materials at the temperature region below T_β has been explored using various techniques, including THz-TDS[24,25] and calorimetric techniques[28]. To date, the majority of THz-TDS studies presented in the literature have investigated small organic molecules or hydrogen bonded systems[26]. This present work systematically examines a number of polymer systems by investigating the behaviour and trends these exhibit as a function of and the values of T_β and $T_{g,\alpha}$ obtained. The purpose of this study is to better understand the relationship between the relaxation dynamics and the molecular structure of PLGA systems that vary in molecular weight (MW) as well as in lactide to glycolide ratio using THz-TDS and DMA. We propose an explanation of the mechanism of the α- and β-relaxation processes in amorphous PLGA.

Finally, we attempt to rationalise the observations of T_β and $T_{g,\alpha}$ in the context of previous theory. We propose an explanation as to why there is a significant change of the respective glass-transition processes for this set of PLGA materials and we discuss our experimental observations in terms of their fundamental origin. We would like to explicitly highlight our notation: in this manuscript we use the symbol $T_{g,\alpha}$ for the temperature where $\tau_\alpha T_{g,\alpha} = 100\,\mathrm{s}$ for the dielectric α-relaxation process and T_β where $\tau_\beta T_\beta = 100\,\mathrm{s}$ for the JG β-relaxation process. In this manuscript we explicitly do not use the term $T_{g,\beta}$ but we would like to emphasise that $T_\beta \equiv T_{g,\beta}$ in the context of our previous work and that of others[7,15,24,26,27,29].

1 EXPERIMENTS

1.1 Sample Preparation

Throughout this work the polymers are referred to by the monomer ratio used: for instance, PLGA 75:25 identifies a copolymer consisting of 75% lactic acid and 25% glycolic acid. Low-MW ($7-17\,\mathrm{kDa}$) and high-MW ($54-69\,\mathrm{kDa}$) PLGA 50:50, low-MW ($4-15\,\mathrm{kDa}$, dispersity, $Đ = 2.5$) high-MW ($76-115\,\mathrm{kDa}$) PLGA 75:25, and medium MW ($18-24\,\mathrm{kDa}$) Poly (D,L lactide) (PDLLA), were purchased from Sigma-Aldrich (Gillingham, United Kingdom). Medium-MW ($10-25\,\mathrm{kDa}$, $Đ = 1.9$) PLGA 50:50 and medium-MW ($20-30\,\mathrm{kDa}$, $Đ = 1.8$) PLGA 75:25 were purchased from Evonik (Birmingham, AL, United States).

For each sample, a sandwich structure consisting of a layer of polymer embedded between two z-cut quartz windows of 13 mm diameter and 2 mm thickness each (Crystran Ltd., Dorset, UK), was formed by vacuum compression moulding (VCM), using the VCM Essentials tool (MeltPrep, Graz, Austria) operating with a circular die of 13 mm inner diameter die. For THz-TDS experiments, the resulting sandwich structure consists of two z-cut quartz windows enclosing the sample, which was separated by a glass fibre reinforced Teflon spacer. The sample thicknesses was adjusted with the spacer and ranged between $300-600\,\mu\mathrm{m}$. Using the VCM Essentials tool, initially, the samples were subjected to vacuum compaction and pre-drying, followed by a vacuum melting step and subsequent cooling and solidification. Suitable temperatures for sample preparation were identified in the range of $408-413\,\mathrm{K}$. Vacuum compaction and pre-drying at room temperature were performed for 3 minutes at 20 mbar. The vacuum melting step to form the quartz/polymer/quartz sandwich moulding structure was completed within an additional 10 minutes under continued vacuum at 20 mbar, allowing for sufficient time for the polymer sample to melt. Then, the VCM tool was manually transferred to the cooling unit of the VCM Essentials setup and the sample was allowed to cool to room temperature for 5 minutes without active cooling. For the DMA experiments, samples were prepared using the VCM bar tool instead of the circular die, at temperatures between $353-373\,\mathrm{K}$ under a pressure of 20 mbar. The samples obtained were approximately 35 mm in length, 12 mm in width, and 0.50 mm in thickness.

1.2 Experimental Setup

The THz-TDS spectra were acquired using a commercial TeraPulse 4000 instrument across the spectral range of $0.2-2.2\,\mathrm{THz}$ (TeraView, Cambridge, UK). The sample temperature ($90-360\,\mathrm{K}$) was controlled using a continuous flow cryostat with liquid nitrogen as the cryogen (Janis ST-100, Wilmington MA, USA) as outlined previously.[29] The cryostat cold finger accommodated both the reference (two z-cut quartz windows) as well as the sample (quartz/sample/quartz sandwich structure as described above).

The two z-cut quartz windows for the reference (same dimensions as sample) were directly pressed to one another without any spacer in between the two windows in order to avoid internal reflections in the time-domain signal. The cold finger was moved vertically using a motorised linear stage to switch between sample and reference at each measurement temperature. For each temperature, the sample and the reference were measured at the centre position, with 2000 waveforms co-averaged for each, for approximately 2 minutes.

The temperature of the sample was measured using a silicon diode mounted to the copper cold finger of the cryostat. The temperature controller used was a Lake Shore model 331 (Westerville, OH, USA). For each series of measurements a sample and a reference were loaded into the cryostat, the cryostat chamber was evacuated to 10 mbar and the cold finger was cooled to a temperature of 90 K. The cryostat was allowed to equilibrate for $10-15$ minutes at 90 K and the first set of sample and reference measurements was acquired. Subsequently the cold finger was heated using temperature intervals of 10 K (at a rate of $2\,\mathrm{K\,min^{-1}}$). At each temperature the system was allowed to equilibrate for 3 minutes before a set of sample and reference measurements were acquired.

In order to further investigate the T_β and $T_{g,\alpha}$ values measured by THz-TDS using a well-established reference method samples of low, medium and high MW PLGA 75:25 as well as medium and high MW PLGA 50:50 were studied using DMA. DMA measurements were performed using the dynamic-mechanical analyser Q800 DMA from TA Instruments (New Castle, De, USA). The oscillation amplitude was set to $20\,\mu$m and the test frequency was held constant at 1 Hz. The DMA measurements were carried out during heating with a temperature sweep covering the range of $138-358$ K. The initial stabilisation time at 138 K was set to 5 minutes, and the heating rate was $3\,\mathrm{K\,min^{-1}}$ with measurements continuously acquired throughout heating of the sample. Two experimental repeats were completed for each material, with a fresh sample prepared before each experimental run.

1.3 Data Analysis

In order to calculate the absorption coefficient and the refractive index of the sample a modified method for extracting the optical constants from terahertz measurements based on the concept introduced by Duvillaret et al. was used[29,30]. The changes in dynamics of the polymer sample were analysed by investigating the change in the absorption coefficient at a frequency of 1 THz as a function of temperature. We have previously demonstrated that discontinuities in the temperature dependent absorption data in disordered materials can be observed that reflect changes in the molecular dynamics of the system[26]. In many cases, including the copolymers studied here, the change in absorption with temperature is linear. At present this linear temperature dependence is merely an empirical observation and it is not fully understood for which systems a linear relationship is to be expected. In the absence of any clear theory to dispute the validity of this approach, we have based our analysis of the experimental data in order to identify the transition points on a linear relationship. Given that the discontinuities between adjacent linear regimes can be rather subtle, we implemented a rigorous fitting routine based on statistical analysis to analyse our data and determine the transition points. Using MATLAB (2016b, The MathWorks, MA, USA), a best fit analysis for each data set was developed to establish the number of regions as well as the corresponding transition points between the different regimes of molecular dynamics. In order to achieve this ,we systematically fitted first two and then three linear regression regions to the data. All co-polymer samples that we examined exhibited regions that could be described by a linear relationship between temperature and terahertz absorption. We observed at least two, and in most cases three, such regions in the temperature range studied with characteristic transition points between them. These discontinuities are indicative of a change in the molecular mobility of the material. For each linear fit, the figures of merit for the fit were calculated and compared. By seeking the minimum mean squared error, we empirically identified the best linear fit to the data, the number of linear regions and the intersection points between neighbouring regions. The slope of the linear fit in each region and the transition temperature, as defined by the intersection point of two adjacent linear fit lines were determined.

For each set of d data points $\{(x_1,y_1),(x_2,y_2)\dots(x_d,y_d)\}$ where x represents the temperature and y represents the absorption coefficient, the model for r linear regions $r=2$ or 3 and $r-1$ intersection points between regions can be described as

$$\hat{y}(x)=\begin{cases} m_1x+b_1 & \text{if } x_1\le x\le x_{i_1} \\ m_2x+b_2 & \text{if } x_{i_1}\le x\le x_{i_2} \\ \vdots & \vdots \\ m_rx+b_r & \text{if } x_{i_{R-1}}\le x\le x_d \end{cases} \tag{1}$$

Here i represents a point of intersection where $i_1<i<i_2...<i_{r-1}<d$, $r\in\mathbb{N}$. m and b are fitting parameters, where m represents the gradient of a region and b represents the y-intercept. The mean squared error MSE $=\sum_{i=1}^{d}\left[(\hat{y}(x_i)-y_i)^2/d\right]$ was minimised by iterating $i_1,i_2,\dots,i_d$ and performing a linear regression over the data points of each region r. The number of linear regions and the range of data points for each region were chosen based on the combination of parameters that resulted in the lowest total MSE for the iterative fitting procedure. The values for m and b and their errors were determined for the linear fits of the respective regions that exhibited the lowest MSE.

In order to analyse the DMA data we applied the following methodology: (1) The data was binned into temperature intervals of 1 K and averaged; (2) the peak position of the local maximum in the $\tan\delta$-curve was determined at low temperatures (below 300 K); (3) the onset value of the peak due to α-relaxation (which in all cases was well separated from the β-process above 300 K) was determined. Here, $\tan\delta$ is defined as the loss tangent, i.e. the ratio of the loss modulus to storage modulus[31]. When determining $T_{g,\alpha}$ in the DMA data we used the onset value of the $\tan\delta$-peak at temperatures above the β-relaxation. This is consistent with the methodology we implement when detecting T_β and $T_{g,\alpha}$ from the THz-TDS data. However, it is not possible to define T_β at low temperatures in terms of its onset value in the

Mode	MDSC		THz-TDS		DMA	
Material	MW (kDa)	$T_{g,\mathrm{DSC}}$ (K)	T_β (K)	$T_{g,\alpha}$ (K)	T_β (K)	$T_{g,\alpha}$ (K)
PLGA 50:50	7 – 17	311	136	302	N/A	N/A
PLGA 50:50	10 – 25	315	233	317	184 – 260	315
PLGA 50:50	54 – 69	326	243	331	164 – 293	320
PLGA 75:25	4 – 15	313	238	317	218 – 282	322
PLGA 75:25	20 – 30	321	179	308	163 – 298	314
PLGA 75:25	76 – 115	320	178	321	177 – 289	318
PDLLA	18 – 24	319	212	298	N/A	N/A

Table 1 Transition temperatures determined by different characterisation techniques. For THz-TDS T_β and $T_{g,\alpha}$ are reported as onset temperatures. For DMA, T_β is reported as the temperature range which the $\tan\delta$ spans below 300 K, and $T_{g,\alpha}$ is reported as an onset temperature.

DMA data, as the DMA instrument cannot acquire data at sufficiently low temperatures to reliably determine the onset of T_β. Therefore, we instead report the range of the temperatures which the $\tan\delta$ peak spans at low temperatures corresponding to the β-relaxation process.

1.4 Modulated Differential Scanning Calorimetry (MDSC)

A Q2000 Differential Scanning Calorimeter (TA Instruments, New Castle, DE, USA) was used to determine the calorimetric glass transition temperature ($T_{g,\mathrm{DSC}}$, defined by the onset temperature) for each material. For each measurement $2-3$ mg of sample material were placed in hermetically sealed aluminium pans under a constant flow nitrogen atmosphere (flow rate 50 ml min^{-1}) and heated at 3 K min^{-1} from room temperature to above the melting temperature T_m, of the material. Following the melt of the polymer, the samples were cooled to approximately 213 K at a rate of 3 K min^{-1} . The samples were subsequently heated again through T_g at a rate of 3 K min^{-1}. The modulation frequency was 0.003 K s^{-1}. The temperature and heat flow of the instrument were calibrated using indium ($T_m = 430$ K, $\Delta H_{\mathrm{fus}} = 29$ J g^{-1}).

2 RESULTS AND DISCUSSIONS

2.1 Temperature Dependence of Terahertz Absorption Coefficient and Dynamic Mechanical Analysis

The calorimetric $T_{g,\mathrm{DSC}}$ was determined for each sample and the resulting values are listed in Table 1. As expected from Fox-Flory theory, we observed an increase in T_g with increasing average MW of the respective polymer samples.

The terahertz spectra of all PLGA materials showed an increase in absorption with frequency and temperature over the entire investigated range, which is in line with previous measurements of disordered molecular solids in general and amorphous polymers in particular (Figure 1a). As expected, no discrete spectral features were present in the frequency range covered by our instrument and the spectra were dominated by the monotonous increase with frequency that is characteristic for the rising flank of the broad peak due to the vibrational density of states (VDOS).[26] In contrast, the refractive index decreases slightly with increasing frequency (see ESI). To further investigate the relationship between the increase of absorption coefficient and temperature

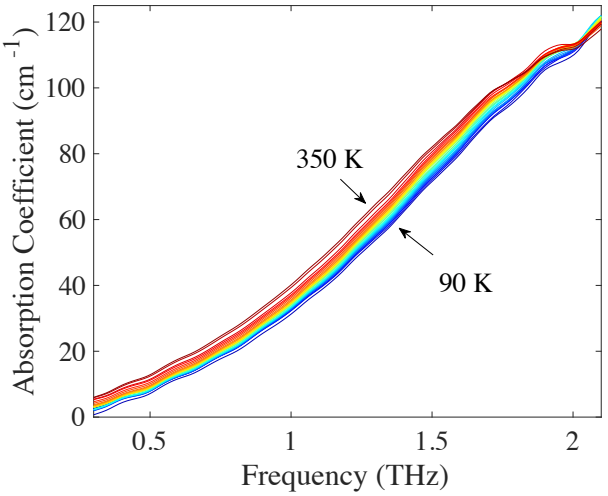

Fig. 1 Absorption coefficient spectra of high MW PLGA 75:25 in the temperature range of $90-350$ K, with 10 K temperature increments between spectra.

we examined the temperature dependent changes in absorption losses at a frequency 1 THz in more detail. Given the lack of distinct spectral features we chose the frequency of 1 THz as the signal-to-noise ratio of the measurement at this frequency is highest for our spectrometer and the absorption is clearly dominated by the VDOS in this spectral region[29].

The changes in absorption at a frequency of 1 THz with temperature for the samples of PLGA 50:50, PLGA 75:25, and PDLLA are plotted in Figures 2 and 3 respectively. It is interesting to note that for the sample of PDLLA the gradient, m, of the linear fit for the first region is steeper compared to that of the second region, which is in contrast to all other samples investigated in this study. For $r = 3$, T_β was defined as the intersection point of the two best-fit linear fits at low temperatures and $T_{g,\alpha}$ was defined as the intersection point of the two best-fit linear lines at high temperatures.

It is well established that the α-relaxation and β-relaxation processes are associated with different molecular motions in the bulk of the polymer material. Overall, the glassy co-polymer chains are more densely packed at low temperatures, compared to at higher temperatures. The onset of T_β corresponds to the lowest temperature at which the co-polymer system is excited with sufficient energy to allow for localised reorientational motion of smaller segments within the co-polymer macromolecule to occur[32]. Thus, at low temperatures, motions which require high activation energies and or large amounts of free volume are restricted.[33]. In contrast, for the α-relaxation this involves the movement of large segments of the copolymer backbone[4]. At temperatures above the glass transition the polymer chains are more loosely packed and sufficient thermal energy is available for the copolymer to cross higher energy barriers, giving rise to the α-relaxation. The motions of the co-polymer chains can therefore be divided into two categories: (1) motions associated with the β-relaxation process that require relatively low activation energy and a small amount of free volume, and (2) motions requiring a large amount of free volume and/or intermolecular activation

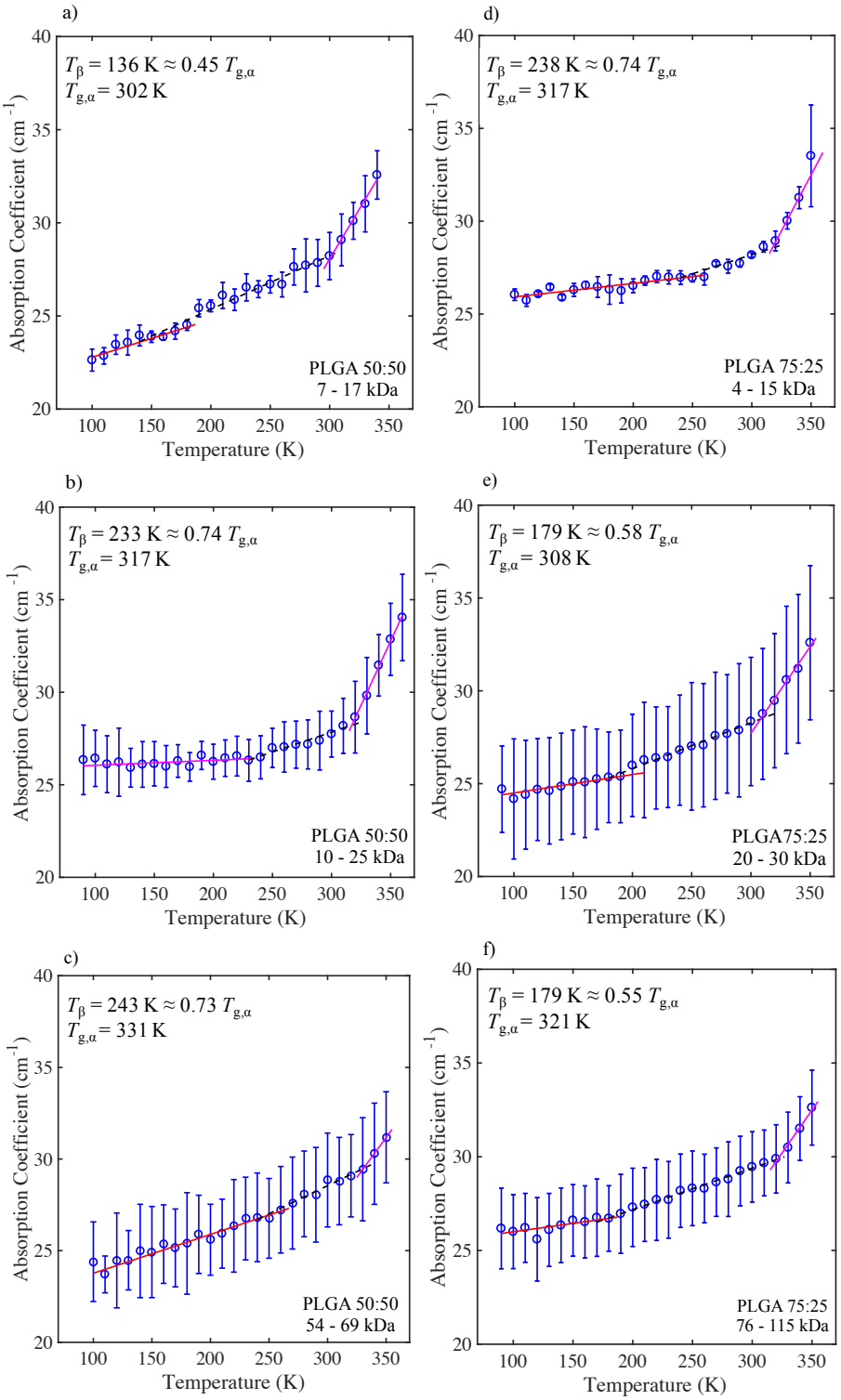

Fig. 2 Mean terahertz absorption coefficient as a function of temperature at 1 THz for PLGA 50:50 a) low, b) medium, and c) high MW. PLGA 75:25 d) low, e) medium, and f) high MW. Lines show the different linear fits for the different regions. Error bars represent the standard deviation for n samples: $n = 3$ for a), d), e), and f), and $n = 4$ for b) and c).

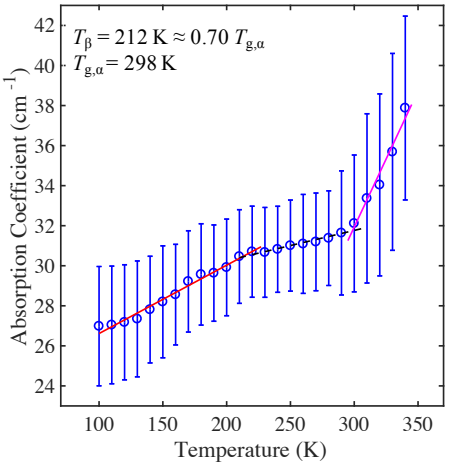

Fig. 3 Mean terahertz absorption coefficient as a function of temperature at 1 THz for a medium MW sample of PDLLA. Lines show the different linear fits for the different regions. Error bars represent the standard deviation for $n = 4$ samples.

energy for the α-relaxation processes.

In the case of the low, medium, and high MW materials of PLGA 50:50 and PLGA 75:25 the change in absorption with temperature can be observed to take place over three distinct regions and two transition temperatures, T_β and $T_{g,\alpha}$, as determined using the methodology outlined above (see Figures 2a and b; Figures 2c and d; and Table 2). In the case of PDLLA again three distinct regions with two transition temperatures are apparent (Figure 3).

For the DMA data, $\tan\delta$ was plotted versus temperature for medium and high MW PLGA 50:50, and for low, medium, and high MW PLGA 75:25, shown in Figure 4. We did not examine the low MW PLGA 50:50 material, as the T_β value of this material, found using the THz-TDS experiments, is below the temperature range which could be measured using the DMA technique, and thus could not be compared. Given that for all the materials studied the $\tan\delta$ peaks at low temperatures are relatively broad, we specify the temperature range over which each $\tan\delta$ peak spans and the maximum value obtained for each $\tan\delta$, β peak, listed in Table 1.

We first attempt to explain the origin of the transition temperatures, corresponding to T_β and $T_{g,\alpha}$, by proposing a physical picture of the change in PLGA dynamics with temperature. Second, we link this physical picture to the concept of free volume in order to offer an understanding of temperature-dependent PLGA dynamics and their contribution to the observed α- and β-relaxation processes. It is worth noting at the outset that the values of $T_{g,\alpha}$, as determined from the THz-TDS experiments, are in good agreement with our own calorimetric measurements, $T_{g,\mathrm{DSC}}$, and our own DMA measurements, $T_{g,\mathrm{DMA}}$, as well as the values reported in the literature for these materials[34].

2.2 Physical Mechanism of Relaxation Process

The structural units of the polymer chain act as a collection of kinetic units such that each is capable of moving independently alongside the cooperative motion of adjacent macromolecular do-

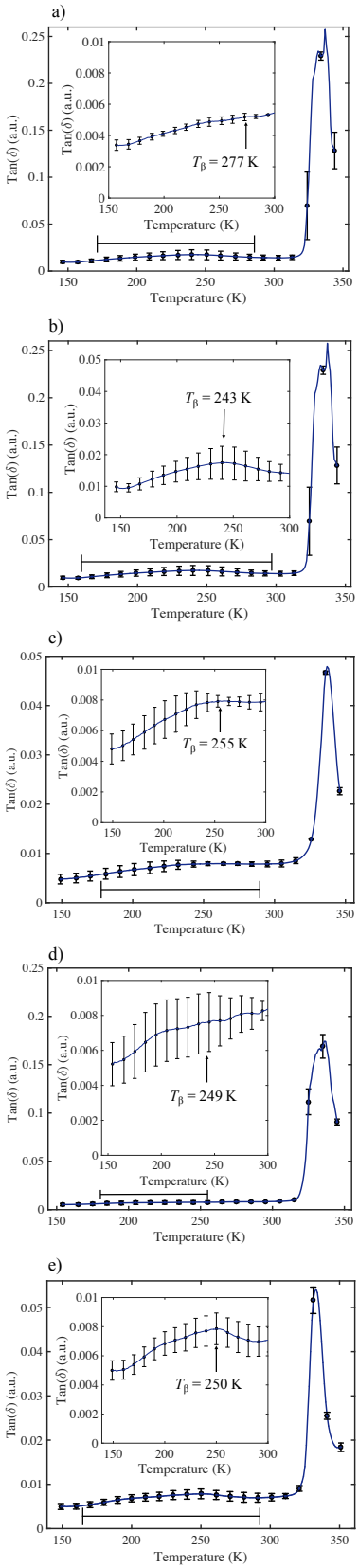

Fig. 4 $\tan\delta$ as a function of temperature for PLGA 75:25 a) low, b) medium, and c) high MW, and for PLGA 50:50 d) medium, e) high. Error bars represent the standard deviation for $n = 2$. For clarity, error bars are shown for every tenth point. The image on the left of each plot shows a zoomed-in view of its $\tan\delta$ peak at low temperatures. The temperature range which the $\tan\delta$ peak spans is indicated by a solid black line.

Material	MW (kDa)	Region 1 ($cm^{-1}K^{-1}$)	Region 2 ($cm^{-1}K^{-1}$)	Region 3 ($cm^{-1}K^{-1}$)
PLGA 50:50	7 – 17 (low)	0.020 ± 0.0025	0.029 ± 0.0024	0.11 ± 0.0069
PLGA 50:50	10 – 25 (med)	0.0027 ± 0.0015	0.022 ± 0.0021	0.14 ± 0.0046
PLGA 50:50	54 – 69 (high)	0.021 ± 0.0013	0.031 ± 0.0026	0.0014 ± 0.0032
PLGA 75:25	4 – 15 (low)	0.0073 ± 0.0011	0.021 ± 0.0046	0.12 ± 0.011
PLGA 75:25	20 – 30 (med)	0.010 ± 0.0016	0.025 ± 0.0012	0.093 ± 0.0066
PLGA 75:25	76 – 115 (high)	0.0089 ± 0.0025	0.022 ± 0.00061	0.091 ± 0.0085
PDLLA	18 – 24 (med)	0.034 ± 0.0014	0.015 ± 0.0018	0.14 ± 0.015

Table 2 Gradient, m, of the linear fit ($y = mx + c$) for the respective temperature regions as outlined in Section 1.3 as well as the respective glass transition temperatures determined based on the terahertz analysis. For high MW PLGA 50:50 and PLGA 75:25 only two regions were identified using the data analysis routine, $r = 2$, whilst for all other samples three regions were found, $r = 3$.

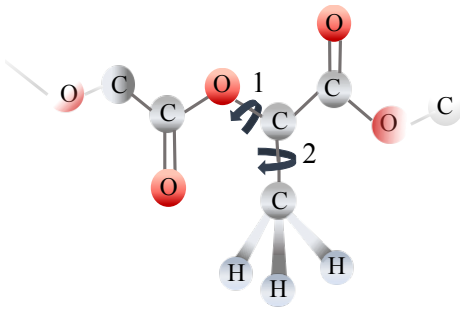

Fig. 5 Chemical structure and molecular motions of an individual segment of PLGA. The motions of PLGA can be described by the rotation of its methyl side groups (indicated by rotation 2) and the the rotations of single C-O bonds, restricted between the he sp^2 hybridized C=O groups (indicated by rotation 1).

mains. The PLGA —$[C_3H_4O_2]_x[C_2H_2O_2]_y$— chains include the methyl side groups of poly(lactic acid) (PLA) and oxygen atoms at every third position of the copolymer backbone (Figure 5). Given the relatively low activation energies, two types of motions are possible for the PLGA chains at low temperatures: (1) the rotation of small polymer segments which include the methyl side groups[11,35–37], and (2) the rotation of small polymer segments which include C-O bonds. The C-O bonds are effective electron donors and contribute a large degree of molecular freedom to the copolymer backbone, thereby enhancing torsional motions in the copolymer backbone (Figure 5, rotation 1). Based on our data, and extensive investigations in the literature[5,9–11,35–37], we hypothesise that the rotational motions of individual polymer segments, described above, and the associated changes in dipole moments are responsible for the observed changes in the terahertz spectra and that the onset of these motions is critical to the β-relaxation process in PLGA. At low temperatures the relative density of the PLGA chain segments is high and the motions of the chain segments are hindered due to their tight packing. The C-C bonds of the PLGA main chain have hydrogen atoms and methyl groups attached that sterically hinder rotation about the C-C bonds. Additionally, the C=O bonds introduce significant structural rigidity to the copolymer chain due to the restricted rotation about the double bonds of a sp^2 hybridised carbon. Therefore, it is likely that at low temperatures small segments including the C-O bonds of PLGA can rotate about the backbone carbon atom of the sp^2 hybridized C=O groups (Figure 5 rotation 1). The change in conformation of individual chain segments requires little free volume and the activation energy of the C-O bond rotation is expected to be low as the conformation is defined by relatively shallow potential energy minima that govern its dihedral angles. This motion could be coupled or accompanied, and indeed facilitated, by the rotational motion of small polymer segments which include the methyl side group 5 (rotation 2 albeit the methyl rotation itself is not infrared active). It is highly conceivable that such motions can readily occur at low temperatures, as the rotational barrier for methyl groups is well known to be rather low, of the order of a few $kJ\,mol^{-1}$ [38]. We believe that it is these types of molecular motion that give rise to T_β of the PLGA materials.

Upon increasing the temperature the density of the copolymer will decrease further due to thermal expansion, which means that in turn the free volume increases. As a result, cooperative motions can gradually take place alongside the more localised motions that are responsible for the β-relaxation process[39–41]. It is commonly accepted that the $T_{g,\alpha}$ coincides with the glass transition and that this process corresponds to the structural relaxation of the polymer[5,42]. With an increase in temperature, segmental co-polymer movement becomes possible, and at the glass transition the dominating motions are likely to be the large-scale chain motions. We believe that these motions give rise to $T_{g,\alpha}$ of the PLGA materials.

2.3 Role of Free Volume

If we consider the macromolecules of amorphous PLGA as a covalently linked assembly of mobile segments where each segment has an associated degree of free movement, the interlacing chains of random molecular arrangement will result in free volume (which is essentially the surplus empty space or voids between the copolymer chains). With increasing free volume the potential energy barriers for the chain segments to change in dihedral angle decrease further, and a wide range of local motions become possible (resulting in the β-relaxation process). Ultimately, the α-relaxation sets in when sufficient free volume and thermal energy for the large amplitude motions of the intermolecular chains is available. Notably, using positron annihilation spectroscopy the free volume hole distribution in a polymer can be measured as a function of temperature[43]. For different glassy polymers, the size distribution broadens with an increase in the

average size of free volume of the polymer[44]. Thus, for the different molecular weight samples of PLGA we would expect different distributions of free volume, with a shift to a broader distribution at temperatures above T_g .

It is interesting to note that we observe a correlation between the average MW of the co-polymer, the lactide to glycolide ratio and T_β and $T_{g,\alpha}$ in PLGA. The Fox-Flory equation is a widely used empirical expression that predicts the behaviour of T_g as a function of average MW[45,46]:

$$T_g = T_{g,\infty} - K/M_n \quad (2)$$

Here $T_{g,\infty}$ is the glass transition temperature for an ideal polymer chain of infinite length, K is a proportionality constant, and M_n is the number average MW of the polymer[47]. The equation reflects that a polymer of low MW has more free volume than a polymer of high MW, since the low MW polymer must have a greater concentration of chain ends for the same mass of sample. Consequently, an increase in the concentration of chain ends is accompanied by a decrease in T_g. For a given polymer, an increase in chain end concentration directly affects the average packing density of the polymer, and the presence of end groups results in a decrease in the density of the configurational structure in proportion to $1/M_n$[45]. For a given dispersity, the constant K is directly related to the free volume of the end groups of polymer chains. A rigid polymer, for example polystyrene, exhibits a strong MW dependance on T_g that is reflected in high values of $T_{g,\infty}$ and K; while a more flexible polymer, such as polydimethylsiloxane, exhibits smaller values of $T_{g,\infty}$ and K and hence the MW dependance on T_g is far weaker[47]. Previous work on PDLLA reported values of $T_{g,\infty} = 330\,\mathrm{K}$ and $K = 7.30 \times 10^4\ \mathrm{K}$[48]. Using these values we find that the Fox-Flory equation yields a predicted $T_{g,\mathrm{theor.}} \approx 326\,\mathrm{K}$, for PDLLA which is in reasonable agreement with our calorimetric measurement of $T_{g,\mathrm{DSC}} = 319\,\mathrm{K}$, yet higher than $T_{g,\alpha} = 298\,\mathrm{K}$ (Table 1).

2.4 Effect of Copolymer Ratio on Molecular Mobility

The THz-TDS data shown in Figure 2 demonstrates that there is a significant dependence of T_β and $T_{g,\alpha}$ on the MW of the PLGA copolymers. As shown by the schematic in Figure 6, for PLGA 50:50 an increase in the MW of the sample results in a decrease of the free volume. (In the THz-TDS data for PLGA 50:50, we observe three regions with a distinct T_β separating the lower temperature regions for each sample (Figures 2a, b, and c). The T_β value of the low MW material ($T_{g,\beta} = 136\,\mathrm{K}$), is significantly lower than that of the medium MW samples ($T_{g,\beta} = 233\,\mathrm{K}$) and of the high MW samples ($T_{g,\beta} = 243\,\mathrm{K}$)). For PLGA 50:50, the long chains of the medium and high MW material entangle with each other far more than the shorter chains of low MW material. Therefore, the higher MW materials have more chain interactions to overcome before the chains can begin moving; and, thus require greater energy and sufficient free volume for the rotational motions to proceed despite chain entanglement occurring, which increases the entropy of these systems and the values of T_β as well as $T_{g,\alpha}$. As temperature is increased, sufficient thermal energy is supplied to the system to overcome local and segmental chain interactions that limit molecular mobility at lower temperatures, thereby increasing the free volume (and mobility). Additionally, the greater chain entanglement associated with the higher MW samples could contribute to the higher barriers of the PES which would explain the raised values of T_β and $T_{g,\alpha}$ with increasing MW.

As shown by the schematic in Figure 6, for PLGA 75:25 an increase in the MW of the sample results in a decrease in the free volume of the system, and consequently, the higher MW PLGA 75:25 materials exhibit a similar behaviour to that of the low MW PLGA 50:50. For all the PLGA 75:25 samples, we observe three distinct regions in the THz-TDS data. Additionally, we observe that low MW PLGA 75:25 (Figure 2c) has a much higher T_β value compared to that of the low MW 50:50 co-polymer. Previous work has shown that an increase in lactic acid monomer (i.e. relatively more methyl groups present) reduces polymer mobility due to the steric hindrance introduced by the methyl side groups[49]. We observe this effect for low MW PLGA 75:25, for which the increased number of methyl side groups effectively restrict the rotations around the C-O bonds in the PLGA backbone which results in an increase in T_β. For the α-relaxation, apart from overcoming potential energy barriers, sufficient free volume is required for large-scale motions to take place. The raised $T_{g,\alpha}$ value of low MW PLGA 75:25 reflect the fact that the steric effects dominate, attributed to the high entanglement of the increased number of methyl groups and the copolymer backbone. As the MW is increased in PLGA 75:25, the values of T_β decrease as the free volume effects on the molecular dynamics start to dominate. For the medium and high MW PLGA 75:25, the increase of methyl side groups, which can freely rotate, disrupt the dense packing of the co-polymer chains, resulting in an increase in available free volume and the molecular mobility of the copolymer backbone (Figure 2d) and (Figure 5, rotation 2). Consequently, this increase in free volume between chains loosens the steric hinderance on the C-O bond rotational motion of the co-polymer backbone and reduce T_β, which is exactly what we observe in medium and high MW PLGA 75:25 (Figure 6). As the polymer segments become more mobile, small, isolated regions of free volume between the individual chains merge into larger regions of free volume, thereby reducing the energy barrier for segmental motions and a lower onset temperature of $T_{g,\alpha}$.

In order to better understand the contribution of the methyl side group of PLA and the effect of free volume on the glass transition behaviour of PLGA, we examined PDLLA. Specifically, in the case of poly(lactic acid) (PLA), previous work has shown that the structure of the polymer chain can have a significant influence on T_g. For example, it was found that the value of T_g (as determined by DSC) is reduced in hyper-branched PLA due to an increase in free volume[50]. Figure 3 shows that the T_β value of PDLLA in our measurement is $212\,\mathrm{K}$ ($T_{g,\beta} = 0.70\,T_{g,\alpha}$), which is lower than the T_β value observed for the PLGA 50:50 material of similar MW. This finding suggests that the presence of the methyl group results in steric hindrance to rotations about the free C-O bonds in PDLLA. Notably, the primary difference between the PDLLA and PLGA 75:25 is that the co-polymer PLGA backbone includes more flexible C-O bonds, which would increase the free volume between the polymer chains[51,52]. Finally, to further investigate the

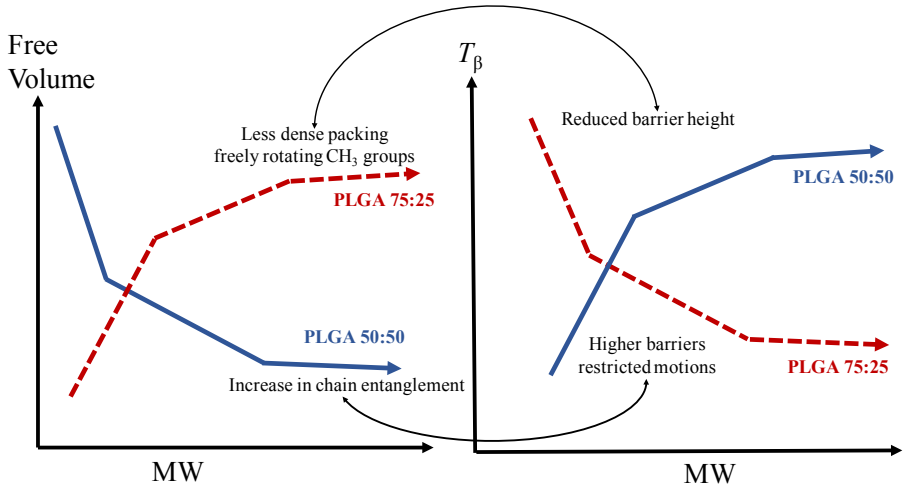

Fig. 6 Behaviour of the different MW material with increasing temperature and free volume. The behaviour of PLGA 50:50 is represented by the blue spheres and solid blue line, and the behaviour of PLGA 75:25 is represented by the red spheres and solid red line. PDLLA is represented by the orange sphere.

T_β and the β-transition, we used DMA to measure the temperature dependence of $\tan\delta$ for samples of low, medium, and high MW PLGA 75:25, and medium and high MW PLGA 50:50, shown in Figures 4, respectively. Both the β- and α-relaxation processes are clearly detected using DMA. At temperatures below 300 K, the β-relaxation process is observed as a broad shallow peak, followed by a sharp peak associated with the α-relaxation. The values of $T_{g,\mathrm{DMA}}$, the onset of the α-relaxation measured by DMA, are in good agreement with the $T_{g,\alpha}$ values obtained from the THz-TDS data (Table 1). Additionally, the storage and loss moduli measured by DMA are in good agreement with the $T_{g,\alpha}$ values obtained from the THz-TDS data (see supplementary materials). It is difficult to compare the β-process measured by DMA compared to that measured by THz-TDS, since we define T_β for the THz-TDS measurements as an onset temperature, but the DMA instrument cannot access sufficiently low temperatures to resolve the onset temperature of the β-process. We therefore report the temperature for the peak of the shallow β-process together with the range of temperatures for the β-process (Table 1). In the context of this discussion it is important to highlight that both the terahertz dielectric measurement as well as the DMA method are measuring the adiabatic process, i.e. the frequency of the measurement is much higher compared to the relaxation time of the process probed in the sample. Notably, we can see similarities between the gradient of the absorption coefficient versus temperature in the THz-TDS data to the $\tan\delta$ of the DMA data. In the DMA data we can see that for low MW PLGA 75:25, T_β is significantly higher compared to that of the medium and high MW PLGA 75:25 materials (shown in Figure 4). This is in good qualitative agreement with the THz-TDS data. The measurements of the β-process for PLGA 50:50 using DMA also agree very well with the THz-TDS experiments (shown in Figure 4): The β-process is observed to shift to higher temperatures with increasing MW. It is worth noting that the strength of the $\tan\delta$ peak in the DMA data has previously been linked with an increase in the freedom of movement of the polymer[53]. We note that the intensity of the $\tan\delta$ peak is increasing with increasing MW, in line with lower molecular mobility in the low MW material compared with the high MW PLGA. In contrast, for high MW PLGA 50:50, the $\tan\delta$ associated with the β-process is not only pronounced but also much broader than that of medium MW PLGA 50:50 (shown in Figure 4). It has been suggested that the width of the $\tan\delta$ peak correlates with the heterogeneity of the environments of the co-polymer and the distribution of mobilities of the polymer chains[31,53]. For the higher MW PLGA 50:50 material, the high chain entanglement leads to more heterogeneous regions in this material compared to the medium MW PLGA 50:50 material, which forms a more homogenous polymer network. This preliminary observation supports the idea that the width of the $\tan\delta$ peak may correlate with the number of heterogeneous environments in the polymer network and in turn the distribution of mobilities of the PLGA chains.

3 CONCLUSIONS

We have studied the dynamic properties and relaxations and glass transition behaviour of PLGA and PDLLA by performing variable temperature THz-TDS measurements. We have shown that the $T_{g,\alpha}$, as measured by THz-TDS, is consistent with the T_g results determined by MDSC for each material. A monotonous increase of absorption coefficient with temperature was observed for all the materials examined. Low, medium, and high MW PLGA 50:50 and PLGA 75:25, and medium MW PDLLA exhibit three temperature regimes, with a distinct transition temperatures T_β and $T_{g,\alpha}$. We rationalise our experimental results with the concepts of free volume and associate T_β with the β-relaxation process, where T_β corresponds to the point at which the material has sufficient amount of thermal energy and free volume for localised motions, here rotations of the C-O bond and methyl side groups, to occur. We conducted DMA measurements in order to further probe the relaxation behaviour of PLGA. We showed that for each of the materials studied, the $\tan\delta$ versus temperature curve shows two

distinct peaks corresponding to the α-relaxation at higher temperatures, and a peak at lower temperatures corresponding to the β-relaxation. Our interpretation of the experimental observations provides a physical explanation to the behaviour of PLGA, based on the PES concept outlined by Goldstein[14]. We attribute the α-relaxation process as the contributing process to $T_{g,\alpha}$, and define $T_{g,\alpha}$ as the point at which the co-polymer structure has further loosened, and with an increase in free volume the long-range segmental motion of the PLGA chains take place. The main novelty of our work concerns the dynamics of the polymer at temperatures below T_g. Whilst Johari and Goldstein were clearly careful to emphasise that there is no merit in trying to ascertain that the β process is originating strictly from either inter- or intra-molecular relaxations, they are explicitly reluctant to incorporate the concept of free volume into their discussion.[12] Our data provides further evidence that the concepts low energy potential energy barriers and free volume are by no means mutually exclusive but that it is intuitive that the increase in free volume with increased temperature directly lowers the heights of the barriers that are primarily inter-molecular in origin. We conclude that in order to conduct a robust analysis of the dynamic response of a copolymer system, such as PLGA, it is necessary to consider the combined effects of both temperature and free volume. Additionally, this work demonstrates that THz-TDS and DMA are effective methods to investigate dynamic processes that affect the behaviour of a co-polymer system.

Supplementary information is provided with this article.

Acknowledgments

The authors acknowledge funding from the UK Engineering and Physical Sciences Research Council (EPSRC, EP/N022769/1). T.A.S. thanks the AJA-Karten Trust and the Kenneth Lindsay Trust for their financial support. Dynamic mechanical analysis was performed at the Department of Pharmacy, University of Copenhagen (UCPH). In particular, the authors appreciate the access to facilities and the help of Professor Thomas Rades and Eric O. Kissi (UCPH) in connection with this work.

Notes and references

1 M. L. Williams, R. F. Landel and J. D. Ferry, *J. Am. Chem. Soc.*, 1955, **77**, 3701–3707.

2 B. C. Hancock, S. L. Shamblin and G. Zografi, *Pharm. Res.*, 1995, **12**, 799–806.

3 G. D. Smith and D. Bedrov, *J. Polym. Sci., Part B: Polym. Phys.*, 2007, **45**, 627–643.

4 H.-B. Yu, W.-H. Wang and K. Samwer, *Mater. Today*, 2013, **16**, 183–191.

5 A. Alegria and J. Colmenero, *Soft Matter*, 2016, **12**, 7709–7725.

6 S. Cerveny, R. Bergman, G. A. Schwartz and P. Jacobsson, *Macromolecules*, 2002, **35**, 4337–4342.

7 A. K. Roy and P. T. Inglefield, *Prog. Nucl. Magn. Reson. Spectrosc.*, 1990, **22**, 569–603.

8 M. D. Barnes, K. Fukui, K. Kaji, T. Kanaya, D. W. Noid, J. U. Otaigbe, V. N. Pokrovskii and B. G. Sumpter, *Advances in Polymer Science Polymer Physics and Engineering*, Springer, Berlin, Heidelberg, Germany, 2001, pp. 317–319.

9 B. Schmidtke, M. Hofmann, A. Lichtinger and E. A. Rössler, *Macromolecules*, 2015, **48**, 3005–3013.

10 C. Chen, J. K. Maranas and V. Garcia-Sakai, *Macromolecules*, 2006, **39**, 9630–9640.

11 V. Arrighi, J. S. Higgins, A. N. Burgess and W. S. Howells, *Macromolecules*, 1995, **28**, 4622–4630.

12 G. P. Johari and M. Goldstein, *J. Chem. Phys.*, 1970, **53**, 2372–2388.

13 G. Williams and D. C. Watts, *Trans. Faraday Soc.*, 1971, **67**, 1971–1979.

14 M. Goldstein, *J. Chem. Phys.*, 1969, **51**, 3728.

15 M. T. Ruggiero, M. Krynski, E. O. Kissi, J. Sibik, D. Markl, N. Y. Tan, D. Arslanov, W. van der Zande, B. Redlich, T. M. Korter, H. Grohganz, K. Lobmann, T. Rades, S. R. Elliott and J. A. Zeitler, *Phys. Chem. Chem. Phys.*, 2017, **19**, 30039–30047.

16 N. Fuse, R. Sato, M. Mizuno, K. Fukunaga, K. Itoh and Y. Ohki, *Jpn. J. Appl. Phys.*, 2010, **49**, 102402.

17 H. Tadokoro, M. Kobayashi, H. Yoshidome, K. Tai and D. Makino, *J. Chem. Phys.*, 1968, **49**, 3359–3373.

18 S. Yamamoto, M. Miyada, H. Sato, H. Hoshina and Y. Ozaki, *J. Phys. Chem. B*, 2017, **121**, 1128–1138.

19 H. K. Makadia and S. J. Siegel, *Polymers*, 2011, **3**, 1377–1397.

20 P. Gentile, V. Chiono, I. Carmagnola and P. V. Hatton, *Int. J. Mol. Sci.*, 2014, **15**, 3640–3659.

21 D. Heiman, D. Hamilton and R. Hellwarth, *Phys. Rev. B*, 1979, **19**, 6583–6592.

22 P. G. Royall, C.-Y. Huang, S.-W. J. Tang, J. Duncan, G. Van-de Velde and M. B. Brown, *Int. J. Pharm.*, 2005, **301**, 181–191.

23 J. M. Carpenter and D. L. Price, *Phys. Rev. Lett.*, 1985, **54**, 441–443.

24 J. Sibik, S. R. Elliott and J. A. Zeitler, *J. Phys. Chem. Lett.*, 2014, **5**, 1968–1972.

25 S. Capaccioli, K. L. Ngai, M. S. Thayyil and D. Prevosto, *J. Phys. Chem. B*, 2015, **119**, 8800–8808.

26 J. Sibik and J. A. Zeitler, *Adv. Drug Deliv. Rev.*, 2016, **100**, 147–157.

27 K. L. Ngai, S. Capaccioli, D. Prevosto and L.-M. Wang, *J. Phys. Chem. B*, 2015, **119**, 12502–12518.

28 D. P. B. Aji and G. P. Johari, *J. Chem. Phys.*, 2015, **142**, 214501.

29 J. Sibik and J. A. Zeitler, *Philos. Mag.*, 2015, **96**, 842–853.

30 L. Duvillaret, F. Garet and J. L. Coutaz, *IEEE J. Sel. Topics Quantum Electron.*, 1996, **2**, 739–746.

31 H. F. Mark and J. I. Kroschwitz, *Encyclopedia of Polymer Science and Technology*, Wiley, Hoboken, United States, 2008, pp. 649–676.

32 S. S. N. Murthy and M. D. Shahin, *Eur. Polym. J.*, 2006, **42**, 715–720.

33 R. N. Haward, *The Physics of Glassy Polymers*, Applied Science Publishers, Barking, United Kingdom, 1973, pp. 34–37, 72, 172–174.

34 H. Keles, A. Naylor, F. Clegg and C. Sammon, *Polym. Degrad.*

Stab., 2015, **119**, 228–241.

35 D. A. Brant, A. E. Tonelli and P. J. Flory, *Macromolecules*, 1969, **2**, 228–235.

36 M. E. Brown and P. K. Gallagher, *Handbook of Thermal Analysis and Calorimetry Recent Advances, Techniques and Applications*, Elsevier, Amsterdam, The Netherlands, 2008, pp. 230–239.

37 K. Schmidt-Rohr, A. S. Kulik, H. W. Beckham, A. Ohlemacher, U. Pawelzik, C. Boeffel and H. W. Spiess, *Macromolecules*, 1994, **27**, 4733–4745.

38 W. C. Hamilton, J. W. Edmonds and A. Trippe, *Discuss. Faraday Soc.*, 1969, **48**, 192–204.

39 H. F. Mark, *Encyclopedia of Polymer Science and Technology, Concise*, Wiley, Hoboken, United States, 3rd edn, 2007, pp. 1264–1268.

40 S. M. Burkinshaw, *Physico-chemical Aspects of Textile Coloration*, Wiley, Chichester, United Kingdom, 2016, pp. 365, 405, 533.

41 J. F. Rabek, *Photodegradation of Polymers: Physical Characteristics and Applications*, Springer, Berlin, Heidelberg, Germany, 1996, pp. 100, 114.

42 K. Kunal, C. G. Robertson, S. Pawlus, S. F. Hahn and A. P. Sokolov, *Macromolecules*, 2008, **41**, 7232–7238.

43 J. Liu, Q. Deng and Y. C. Jean, *Macromolecules*, 1993, **26**, 7149–7155.

44 D. Hofmann, M. Heuchel, Y. Yampolskii, V. Khotimskii and V. Shantarovich, *Macromolecules*, 2002, **35**, 2129–2140.

45 T. G. Fox and P. J. Flory, *J. Appl. Phys.*, 1950, **21**, 581–591.

46 R. P. White and J. E. G. Lipson, *Macromolecules*, 2016, **49**, 3987–4007.

47 L. Zhang, J. A. Marsiglio, T. Lan and J. M. Torkelson, *Macromolecules*, 2016, **49**, 2387–2398.

48 K. Jamshidi, S. H. Hyon and Y. Ikada, *Polym. J.*, 1988, **29**, 2229–2234.

49 B. Zhu, J. Li, Y. He, H. Yamane, Y. Kimura, H. Nishida and Y. Inoue, *J. Appl. Polym. Sci.*, 2004, **91**, 3565–3573.

50 L. M. Pitet, S. B. Hait, T. J. Lanyk and D. M. Knauss, *Macromolecules*, 2007, **40**, 2327–2334.

51 F. Bueche, *J. Chem. Phys.*, 1953, **21**, 1850–1855.

52 J. D. Ferry, *Viscoelastic Properties of Polymers*, Wiley, New York, United States, 3rd edn, 1980, pp. 280–299.

53 K. Bandzierz, L. A. E. M. Reuvekamp, J. Dryzek, W. K. Dierkes, A. Blume and D. Bielinski, *Materials*, 2016, **9**, year.